




# Host-Derived Metabolites Modulate Transcription of *Salmonella* Genes Involved in L-Lactate Utilization during Gut Colonization

Caroline C. Gillis,<sup>a</sup> Maria G. Winter,<sup>a</sup> Rachael B. Chanin,<sup>a</sup> Wenhan Zhu,<sup>a</sup> Luisella Spiga,<sup>a</sup>  Sebastian E. Winter<sup>a</sup>

<sup>a</sup>Department of Microbiology, University of Texas Southwestern Medical Center, Dallas, Texas, USA

**ABSTRACT** During *Salmonella enterica* serovar Typhimurium infection, host inflammation alters the metabolic environment of the gut lumen to favor the outgrowth of the pathogen at the expense of the microbiota. Inflammation-driven changes in host cell metabolism lead to the release of L-lactate and molecular oxygen from the tissue into the gut lumen. *Salmonella* utilizes lactate as an electron donor in conjunction with oxygen as the terminal electron acceptor to support gut colonization. Here, we investigated transcriptional regulation of the respiratory L-lactate dehydrogenase LldD *in vitro* and in mouse models of *Salmonella* infection. The two-component system ArcAB repressed transcription of L-lactate utilization genes under anaerobic conditions *in vitro*. The ArcAB-mediated repression of *lldD* transcription was relieved under microaerobic conditions. Transcription of *lldD* was induced by L-lactate but not D-lactate. A mutant lacking the regulatory protein LldR failed to induce *lldD* transcription in response to L-lactate. Furthermore, the *lldR* mutant exhibited reduced transcription of L-lactate utilization genes and impaired fitness in murine models of infection. These data provide evidence that the host-derived metabolites oxygen and L-lactate serve as cues for *Salmonella* to regulate lactate oxidation metabolism on a transcriptional level.

**KEYWORDS** *Salmonella*, gut inflammation, microbiome

*Salmonella enterica* serovar Typhimurium is an enteric pathogen that causes sub-acute, self-limiting gastroenteritis in the immunocompetent host (1). *S. Typhimurium* virulence is primarily mediated by two distinct type 3 secretion systems. The type 3 secretion system encoded by *Salmonella* pathogenicity island 1 (2) enables *S. Typhimurium* to invade cultured epithelial cells and the mucosa of infected animals (3, 4). A second type 3 secretion system, encoded by *Salmonella* pathogenicity island 2, enables intracellular replication inside of macrophages (5, 6) and is required for full virulence in murine and bovine models of infection (7–9). Both type 3 secretion systems are required for efficient induction of host inflammatory responses. Development of inflammation drives changes in the microbiota composition (dysbiosis), including an expansion of the pathogen population (10, 11). Increased colonization of the intestinal tract by *Salmonella* enhances fecal shedding and host transmission through the fecal-oral route (12, 13).

The onset of intestinal inflammation changes the metabolic environment of the gut. Recent studies have shown that inflammation leads to the production of the terminal electron acceptors nitrate (14, 15) and tetrathionate (16), as well as leakage of oxygen from host tissue into the gut lumen (13). The availability of electron acceptors supports the outgrowth of *S. Typhimurium*, which is capable of anaerobic and aerobic respiration. In contrast, the microbiota mostly consists of obligate anaerobes that cannot use these electron acceptors. Exogenous electron acceptors allow *S. Typhimurium* to run a complete, oxidative tricarboxylic acid cycle (17). This in turn facilitates the catabolism of poorly fermentable carbon sources, such as ethanolamine and succinate (17, 18).

**Citation** Gillis CC, Winter MG, Chanin RB, Zhu W, Spiga L, Winter SE. 2019. Host-derived metabolites modulate transcription of *Salmonella* genes involved in L-lactate utilization during gut colonization. *Infect Immun* 87:e00773-18. <https://doi.org/10.1128/IAI.00773-18>.

**Editor** Manuela Raffatellu, University of California San Diego School of Medicine

**Copyright** © 2019 American Society for Microbiology. All Rights Reserved.

Address correspondence to Sebastian E. Winter, [Sebastian.Winter@UTSouthwestern.edu](mailto:Sebastian.Winter@UTSouthwestern.edu).

**Received** 12 October 2018

**Returned for modification** 30 October 2018

**Accepted** 2 January 2019

**Accepted manuscript posted online** 7 January 2019

**Published** 25 March 2019

Recently, we have shown that host-derived L-lactate serves as a nutrient source during *S. Typhimurium* expansion in the inflamed gut (19).

Under homeostatic conditions, nondigestible polysaccharides are fermented into the short-chain fatty acid butyrate by members of the class *Clostridia*. Butyrate is oxidized as the primary carbon and energy source for intestinal epithelial cells, a process which consumes oxygen and which keeps the gut lumen anaerobic (20, 21). Butyrate is also a cue for the transcription factor PPAR $\gamma$ , which controls the central metabolism of epithelial cells and drives their metabolism toward oxidative metabolism (13, 19, 22). During *S. Typhimurium* infection, inflammation results in a depletion of butyrate-producing *Clostridia* from the gut as a part of gut microbiota dysbiosis (10, 13). Butyrate deprivation alters host cell metabolism, leading to leakage of oxygen and L-lactate into the gut lumen (13, 19). The respiratory L-lactate dehydrogenase LldD facilitates degradation of host-derived L-lactate in a stereospecific manner (19). The terminal electron acceptor for L-lactate utilization is host-derived oxygen, as lactate oxidation is entirely dependent on the cytochrome *bd* oxidase CydAB (19). Since L-lactate and oxygen become available in the gut through the same mechanism, i.e., inflammation-associated changes in host metabolism, lactate oxidation by the LldD-CydAB electron transport chain constitutes a disease-specific metabolic module that contributes to *S. Typhimurium* outgrowth through manipulation of host metabolism (19).

Here, we investigated how L-lactate utilization is regulated during *S. Typhimurium* infection in the murine gut. LldD is encoded in an operon that contains other genes with putative functions in L-lactate utilization. The first gene in the operon, *lldP*, encodes a putative L-lactate permease. The second gene, *lldR*, encodes a putative regulatory protein. The gene products of *lldPRD* in *S. Typhimurium* 14028 exhibit considerable sequence identity at the amino acid level to the orthologues in *Escherichia coli* K-12 MG1665 (94%, 86%, and 94% for *lldP*, *lldR*, and *lldD*, respectively). While some work has been done to understand the regulation of the homologous operon in *E. coli* under *in vitro* conditions (23, 25, 26), the regulation of the L-lactate utilization operon in *S. Typhimurium*, especially *in vivo*, remains largely uncharacterized. Our results from *in vitro* experiments and murine models of colitis indicate that host-derived oxygen and L-lactate induce transcription of L-lactate utilization genes, suggesting that sensing of these host-derived metabolites governs transcriptional control of the *lldPRD* operon.

## RESULTS

**Oxygen, nitrate, and L-lactate induce lactate utilization genes.** To investigate expression of the *S. Typhimurium* *lldPRD* operon, we first analyzed transcription of individual genes in response to key host-derived metabolites *in vitro*. Mucin broth containing L-lactate or the electron acceptor nitrate was inoculated with an *S. Typhimurium* wild-type strain (IR715). After 3 h of growth under microaerobic or anaerobic conditions, we extracted bacterial RNA and evaluated transcription of *lldP*, *lldR*, and *lldD* by reverse transcription (RT)-quantitative PCR (qPCR) (Fig. 1). In the absence of exogenous electron acceptors, addition of L-lactate alone was insufficient to induce transcription of *lldP*, *lldR*, and *lldD*. In contrast, addition of the electron acceptors oxygen and nitrate was sufficient to significantly upregulate expression by more than 10-fold. Exposure to L-lactate in the presence of oxygen further increased transcription beyond that induced by the electron acceptor alone, up to about 100-fold over that under uninduced conditions (Fig. 1). In addition to LldD, *S. Typhimurium* expresses a second respiratory lactate dehydrogenase termed Dld (27). Unlike LldD, Dld is specific for D-lactate (19). Under the conditions tested, *dld* was not inducible by oxygen, nitrate, or L-lactate (see Fig. S1 in the supplemental material).

Previous reports suggest that under inflammatory conditions, the gut environment becomes microaerobic (13, 22). We thus analyzed how various levels of oxygenation affected *lldD* transcription with no L-lactate and 20 mM L-lactate in lysogeny broth (LB) (Fig. 2A). For this experiment, we created a transcriptional fusion of the *lldD* gene and

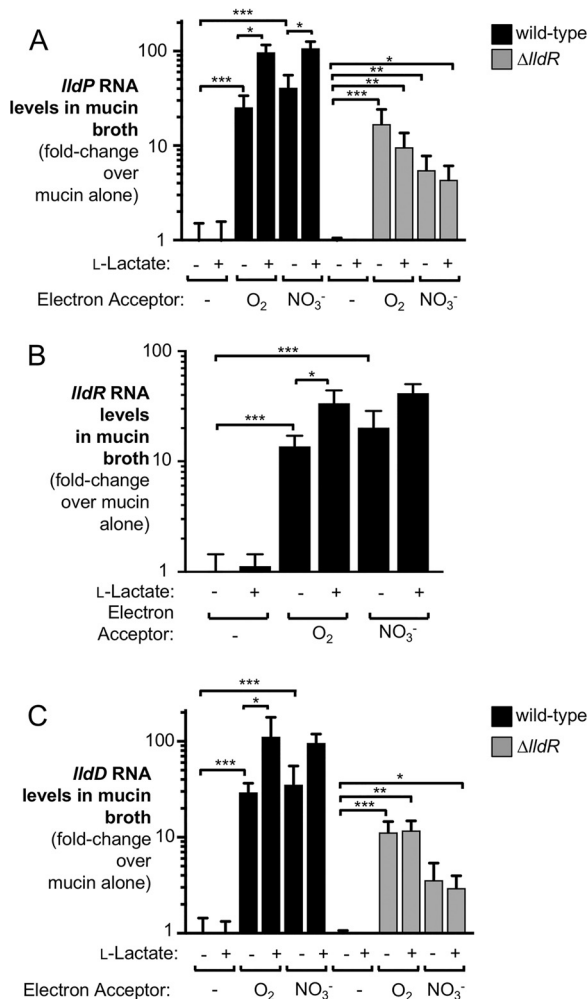


**FIG 1** Analysis of *IldPRD* transcription in response to various stimuli *in vitro*. The *S. Typhimurium* wild-type strain and a  $\Delta IldR$  mutant strain were grown in mucin broth. Nitrate ( $NO_3^-$ ) and L-lactate were added as indicated at concentrations of 40 mM and 20 mM, respectively. Cultures were grown for 3 h anaerobically (no electron acceptor and nitrate conditions) or in the presence of 1% oxygen. RNA was extracted, and *IldP* (A), *IldR* (B), and *IldD* (C) mRNA levels were assessed by RT-qPCR. Transcription was normalized to that of the housekeeping gene *gmk*. All experiments were conducted with at least 3 biological replicates. To determine differences between groups, a two-tailed, unpaired Student's *t* test on ln-transformed data was used. Bars indicate the geometric mean  $\pm$  standard error. \*,  $P < 0.05$ ; \*\*,  $P < 0.01$ ; \*\*\*,  $P < 0.001$ .

*lacZ* (CG254), leaving the coding sequence of *IldD* intact to avoid any changes in expression due to the absence of *IldD*. We exposed cultures of *S. Typhimurium* CG254 to 0% (anaerobic), 1% (microaerobic), 8% (tissue oxygenation), and 21% (atmospheric) oxygen and assessed *IldD* transcription in a standard  $\beta$ -galactosidase assay. Increasing levels of oxygen correlated with increased *IldD* expression, with 21% oxygen inducing the strongest response. Addition of 20 mM L-lactate further increased expression in the presence of oxygen.

**The two-component system ArcAB represses *IldD* expression in the absence of oxygen.** ArcB is a sensor kinase that detects the redox state of the quinone pool and phosphorylates the response regulator ArcA. Phosphorylated ArcA then regulates the transcription of a wide variety of genes (28). In *E. coli*, the ArcAB two-component system represses lactate utilization genes (25, 26, 29, 30). In *S. Typhimurium*, *IldP* and *IldR* were also found to be repressed under anaerobic conditions in a broad survey of the ArcA regulatory program (28). We thus hypothesized that ArcAB would also be involved in the regulation of *IldD*. To test this idea, we compared *IldD* expression in the wild-type

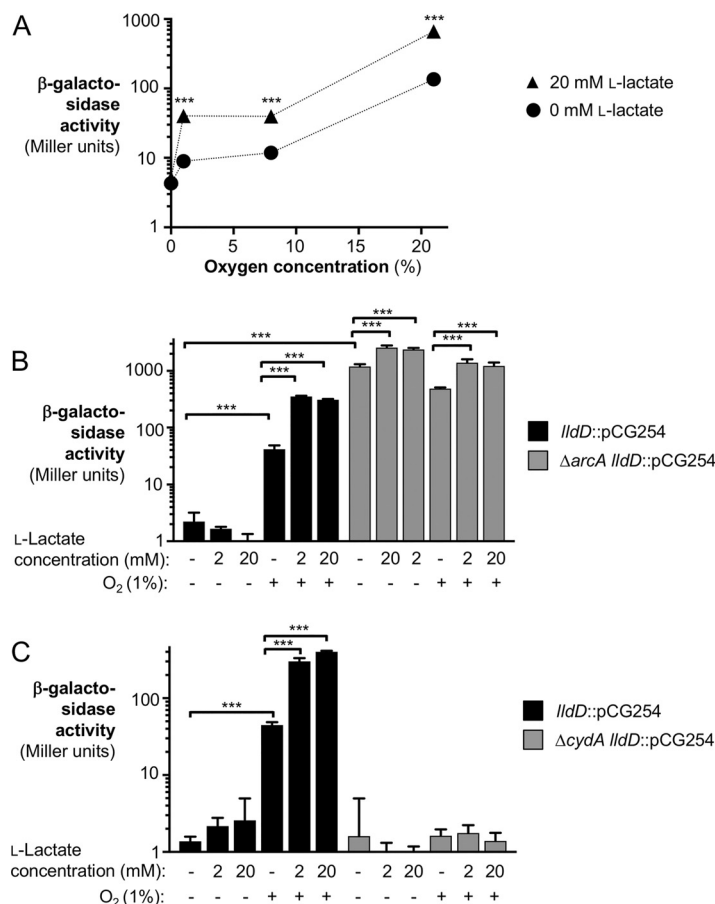


**FIG 2** Influence of oxygen levels, ArcAB regulation, and CydAB-mediated respiration on *lldD* transcription. (A) The *lldD-lacZ* transcriptional reporter strain CG254 (*lldD::pCG254*) was grown in LB in the presence of various concentrations of oxygen. The medium was supplemented with 20 mM L-lactate or mock treated. After 135 min,  $\beta$ -galactosidase activity was quantified. Note that the size of the error bar is smaller than the symbol representing the geometric mean. (B and C) *S. Typhimurium* strains CG254 (*lldD::pCG254*), CG267 ( $\Delta arcA lldD::pCG254$ ), and CG270 ( $\Delta cydA lldD::pCG254$ ) were grown anaerobically (no-oxygen conditions) or with 1% oxygen in LB supplemented with L-lactate, as indicated. After 5 h,  $\beta$ -galactosidase activity was determined. (B)  $\beta$ -Galactosidase activity in the wild-type background and a  $\Delta arcA$  mutant background. (C)  $\beta$ -Galactosidase activity in the wild-type background and a  $\Delta cydA$  mutant background. All experiments were conducted with at least 3 biological replicates. To determine differences between groups, a two-tailed, unpaired Student's *t* test was applied to the ln-transformed data. Bars indicate the geometric mean  $\pm$  standard error. \*\*\*,  $P < 0.001$ .

background (CG254) with that in strains which lack ArcA (CG267) or ArcB (CG268). LB supplemented with and without L-lactate was inoculated with the indicated strains and incubated anaerobically or microaerobically. Since the  $\Delta arcA$  and  $\Delta arcB$  mutants displayed a slight growth defect under aerobic conditions, the cultures were incubated for 5 h. *lldD* expression was then evaluated by  $\beta$ -galactosidase assay (Fig. 2B and S2). Under anaerobic conditions, the wild-type strain had minimal *lldD* expression, even in the presence of L-lactate, while transcription was induced under the oxygenated condition as well as in the presence of oxygen and L-lactate. In contrast, the transcription of *lldD* in the  $\Delta arcA$  and  $\Delta arcB$  mutants was derepressed, and induction by oxygen was lost entirely (Fig. 2B and S2). Of note, these strains still exhibited significant induction by the addition of L-lactate both in the presence and in the absence of oxygen. Taken together, these experiments suggest that ArcAB is responsible for transcriptional repression of *S. Typhimurium lldD* under anaerobic conditions.

**The terminal oxidase CydAB is necessary for *lldD* expression under microaerobic conditions.** In our previous study, we found that L-lactate utilization was dependent on the activity of the terminal oxidase CydAB *in vivo* (19). ArcB senses

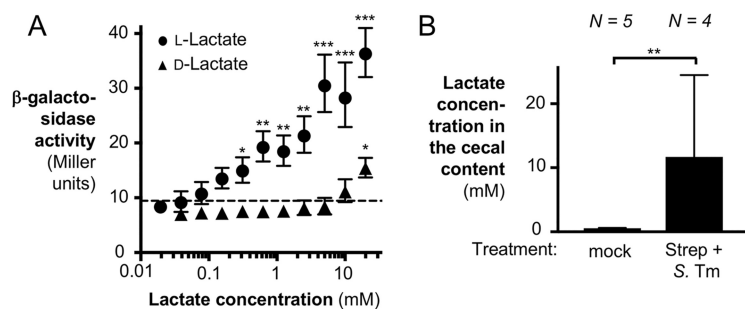


**FIG 3** Analysis of *IldPRD* transcription in response to various concentrations of L-lactate and D-lactate. (A) The *IldD-lacZ* transcriptional reporter strain CG254 (*IldD::pCG254*) was grown in LB for 135 min in the presence of 1% oxygen with various concentrations of L-lactate or D-lactate. *IldD* transcription was assessed by determination of  $\beta$ -galactosidase activity. The dashed line indicates the  $\beta$ -galactosidase activity in the absence of lactate. All experiments were conducted with at least 3 biological replicates. Note that in some instances, the size of the error bar is smaller than the symbol representing the geometric mean. (B) C57BL/6 mice were treated intragastrically with streptomycin, followed by infection with the *S. Typhimurium*  $\Delta IldD$  mutant (CG6) 1 day later (Strep + *S. Tm*). Mock-treated mice (mock) received water, followed by LB 1 day later. The cecal content was collected 5 days after infection for lactate quantification by GC-MS. To determine differences between groups, a two-tailed, unpaired Student's *t* test on ln-transformed data was used. Bars and symbols indicate the geometric mean  $\pm$  standard error. \*,  $P < 0.05$ ; \*\*,  $P < 0.01$ ; \*\*\*,  $P < 0.001$ .

electron flux via the redox state of the quinone pool (31), and thus, we hypothesized that aerobic respiration would contribute to derepression of *IldD*. To test this, we performed  $\beta$ -galactosidase assays as described above using a mutant strain which lacks the terminal oxidase *CydAB* (CG270) (Fig. 2C). While the wild-type strain had increased *IldD* transcription with the addition of oxygen and oxygen with L-lactate, the  $\Delta cydA$  mutant exhibited no increase in *IldD* transcription in the presence of oxygen. Our data suggest that under microaerobic conditions, the electron flux mediated by *CydAB* is sensed by *ArcAB*, which in turn enables *IldD* expression.

**Induction of *IldD* transcription occurs at physiological levels of lactate.** In our previous work, we showed that lactate levels in the murine gut vary considerably (19). The experiments described thus far have used an initial concentration of 20 mM L-lactate. To test if lactate utilization genes were still induced *in vitro* at physiologically relevant concentrations of L-lactate, we performed a dose-response experiment with 1% oxygen and various concentrations of L-lactate (Fig. 3A). There was a significant, dose-dependent increase in the level of *IldD* transcription over that of the oxygen-only condition (dashed line) for a large number of L-lactate concentrations ranging from 0.3125 mM to 20 mM L-lactate.

Next, we analyzed the lactate concentrations in the murine gut lumen during *S. Typhimurium* infection. Streptomycin-pretreated C57BL/6 mice were intragastrically inoculated with the *S. Typhimurium*  $\Delta IldD$  mutant, and the lactate concentrations in the cecal content were quantified by gas chromatography-mass spectrometry (GC-MS). Consistent with our previous results (19), the lactate concentration in mock-treated animals (no streptomycin or *S. Typhimurium* treatment) was approximately 0.6 mM (Fig. 3B). Lactate levels in the *Salmonella*-infected animals rose to about 11.7 mM (Fig. 3B). As such, the responsiveness of *IldD* transcription to lactate *in vitro* (Fig. 3A) encompasses the relevant *in vivo* concentrations of lactate (Fig. 3B).

Host cells produce the L-enantiomer of lactate. To determine the potential contribution of D-lactate to the induction of *IldD* expression, we repeated this experiment with various concentrations of the D-enantiomer (Fig. 3A). In contrast to our previous results with L-lactate, exposure to D-lactate did not increase *IldD* expression significantly, with the exception of exposure to D-lactate at 20 mM, the highest concentration tested. The commercially available D-lactate compound is 98% enantiopure, and thus, the 20 mM D-lactate condition likely contains 0.4 mM L-lactate, which would be sufficient to induce expression. As such, the observed increase in *IldD* expression with 20 mM D-lactate was likely a reflection of this impurity (Fig. 3A).

**The transcriptional regulator LldR enables the response to L-lactate *in vitro*.**

The L-lactate utilization operon includes the putative transcriptional regulator LldR. In *E. coli*, LldR has been shown to increase transcription of L-lactate utilization genes (23, 25). Given that the L-lactate utilization genes in *S. Typhimurium* are also inducible by L-lactate in the presence of electron acceptors, we hypothesized that LldR could also be responsible for the increase in *lldPD* expression in the presence of lactate. To test this, we evaluated transcription of *lldP* and *lldD* in a  $\Delta$ *lldR* mutant (Fig. 1A and C, gray bars). Unlike the wild-type strain, the  $\Delta$ *lldR* mutant was unable to increase transcription of *lldP* and *lldD* when L-lactate was added to the medium, even in the presence of oxygen and nitrate. These data strongly support the idea that the increase in *lldPD* expression in the presence of L-lactate is mediated by LldR.

**LldR mediates *lldPD* transcription in the murine gut.** We next sought to examine transcription of *lldPRD* *in vivo* in a mouse model of *Salmonella* infection. One of the pathological features of nontyphoidal salmonellosis is the development of a neutrophilic infiltrate into the intestinal mucosa (32, 33). Transmigrated neutrophils and other leukocytes are frequently detected in the feces of patients (34, 35). The streptomycin-treated C57BL/6 mouse model has been used extensively by numerous groups as it allows the reproducible colonization of C57BL/6 mice and neutrophils infiltrate the intestinal mucosa upon oral *S. Typhimurium* infection (36). Perturbation of the microbiota by streptomycin prior to *S. Typhimurium* infection ensures the depletion of *Clostridia* and leads to lactate production by the host (Fig. 3B) and leakage of oxygen into the gut lumen (13, 19, 22). Therefore, we initially chose to assess transcription of genes required for lactate utilization in the streptomycin-treated C57BL/6 mouse model. To assess how *lldP* transcription occurs in the murine cecum, we treated wild-type C57BL/6 mice with streptomycin sulfate by oral gavage. One day later, we intragastrically infected mice with an *S. Typhimurium* wild type (IR715), a  $\Delta$ *lldR* mutant (CG200), or a  $\Delta$ *lldD* mutant (CG6). Five days after infection, the mice were sacrificed and the cecal contents were collected for bacterial RNA extraction and RT-qPCR (Fig. 4A to C). We were initially concerned that members of the gut microbiota express genes similar to *S. Typhimurium lldPRD*, thus possibly interfering with our RT-qPCR assay. However, no *lldR* or *lldD* mRNA was detected in mice infected with the *S. Typhimurium*  $\Delta$ *lldR* or  $\Delta$ *lldD* mutant (Fig. 4A to C), respectively, demonstrating that the RT-qPCR assay is specific for the intended *S. Typhimurium* mRNA targets. Similarly, no *lldP* transcription was detected in mice infected with a  $\Delta$ *lldP* mutant (Fig. S3). mRNA for all three genes of the *lldPRD* operon was detected during *S. Typhimurium* colonization of the cecal lumen. Consistent with our *in vitro* data showing that LldR is required for full expression of L-lactate utilization genes in the presence of L-lactate, expression of *lldD* was decreased in the  $\Delta$ *lldR* mutant ( $P < 0.01$ ). A similar trend was observed for *lldP*; however, this decrease was not statistically significant. Intriguingly, *lldP* and *lldR* expression increased in the  $\Delta$ *lldD* mutant (Fig. 4A and B). We speculate that this was due to an accumulation of lactate within the cell, as the  $\Delta$ *lldD* mutant cannot degrade lactate. To ensure that differences in *lldPRD* expression were not due to attenuation of the mutant strains, we analyzed inflammatory cytokines in cecal tissue, which revealed significant inflammation in the streptomycin-treated, *S. Typhimurium*-infected cecum. Inflammation levels were similar across all groups, with the exception of mice infected with the  $\Delta$ *lldD* mutant, which exhibited somewhat lower *Nos2* and *Cxcl1* expression (Fig. S4).

**LldR is required for optimal fitness in the intestinal tract.** We next wanted to explore the contribution of LldR to the fitness of *S. Typhimurium in vivo*. To do this, we assessed the role of LldR in Swiss Webster mice. Swiss Webster mice do not require antibiotic pretreatment to develop neutrophilic inflammation, and thus, the perturbation of the microbiota that occurs is dependent on *S. Typhimurium* virulence factors and not direct killing of the microbiota by antibiotics (19). To determine if LldR provides a fitness advantage in the murine gut, we performed competitive colonization experiments (Fig. 4D). Groups of Swiss Webster mice were intragastrically inoculated with an

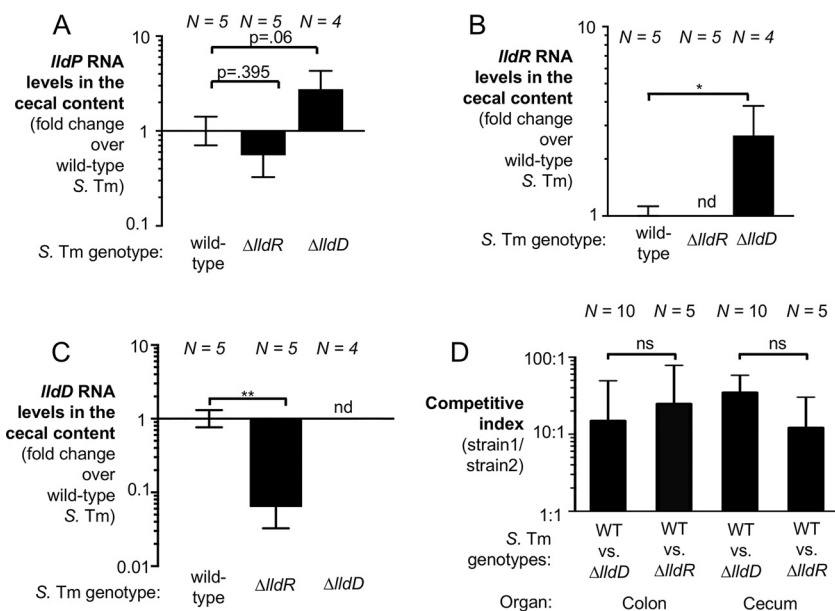


**FIG 4** Effect of LldR on *S. Typhimurium* (*S. Tm*) *lldPRD* transcription and fitness *in vivo*. (A to C) Groups of wild-type C57BL/6 mice were treated with streptomycin by oral gavage. One day later, animals were intragastrically infected with the *S. Typhimurium* wild-type strain (IR715), a  $\Delta lldD$  mutant (CG6), or a  $\Delta lldR$  mutant (CG200). Cecal content was collected for RNA extraction 5 days after infection. *S. Typhimurium* RNA levels were assessed for *lldP* (A), *lldR* (B), and *lldD* (C). Transcription was normalized to that of *S. Typhimurium* 16S rRNA. (D) Swiss Webster mice were inoculated with a 1:1 ratio of an *S. Typhimurium* wild-type (WT) strain (AJB715) and a  $\Delta lldD$  mutant (CG6) or the wild-type strain (AJB715) and a  $\Delta lldR$  mutant (CG200). Colonic and cecal contents were collected 8 days after infection. Wild-type and mutant populations were enumerated on selective agar, and the competitive index was calculated. The number of mice per group (*N*) is indicated for each bar. To determine differences between groups, a two-tailed, unpaired Student's *t* test was applied to the ln-transformed data. Bars are the geometric mean  $\pm$  standard error. \*,  $P < 0.05$ ; \*\*,  $P < 0.01$ ; nd, not detected; ns, not significant.

equal ratio of the *S. Typhimurium* wild type (AJB715) and a  $\Delta lldD$  mutant (CG6) or the *S. Typhimurium* wild-type (AJB715) and a  $\Delta lldR$  mutant (CG200), and the abundance of these strains in the cecal and colonic contents was determined 8 days after infection. As we have shown before, the  $\Delta lldD$  mutant was recovered in lower numbers than the wild-type strain. Similarly, LldR also provided a significant fitness advantage in both the colon and the cecum contents. The competitive fitnesses for the  $\Delta lldD$  mutant and the  $\Delta lldR$  mutant were not significantly different from one another. We also attempted to analyze the transcription of *lldD* in this mouse model. *S. Typhimurium* gut colonization was considerably lower in Swiss Webster mice than in streptomycin-treated C57BL/6 mice, which prevented us from reproducibly quantifying *lldD* transcription in the Swiss Webster mouse model. Collectively, these data suggest that LldR regulates L-lactate utilization on the transcriptional level *in vivo* and that LldR-mediated regulation contributes to optimal gut colonization.

## DISCUSSION

While the majority of *Salmonella enterica* serovars are associated with gastroenteritis, a subset of serovars causes disseminated disease, such as typhoid and paratyphoid fever. The genomes of extraintestinal serovars typically exhibit an increased accumulation of pseudogenes compared to the genomes of intestinal serovars (37, 38), which may reflect adaptations to different niches within the host (39). We have shown previously that *S. Typhimurium* exploits changes in host metabolism, such as the release of oxygen and L-lactate into the gut lumen (Fig. 5) (13, 19). Our data suggest that the inducibility of the *lldPRD* operon by L-lactate may be a specific adaptation to changes in mammalian L-lactate production during infection with the intestinal *Salmonella* serovar Typhimurium. Consistent with this idea, *lldP* and *lldR* were identified to be pseudogenes in the extraintestinal serovars *Salmonella enterica* serovar Gallinarum

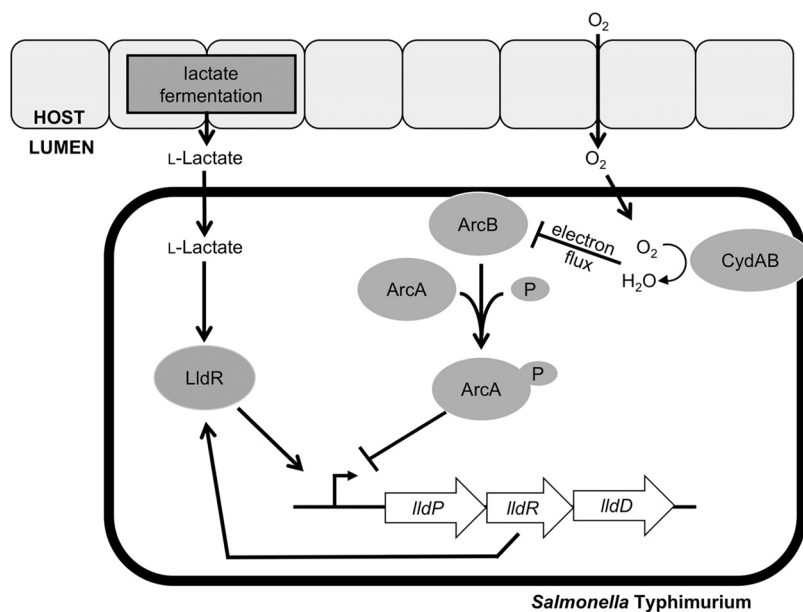


**FIG 5** Central model of regulation of lactate utilization during *S. Typhimurium* infection. Refer to the text for details.

and *Salmonella enterica* serovar Choleraesuis, respectively (37, 40, 41). Furthermore, during experimental *S. Typhimurium* infection of mice, LldD contributes gut colonization but is dispensable for fitness at systemic sites (19).

Our results indicate that the regulation of the *lldPRD* operon is stereospecific to L-lactate. Mammalian cells produce L-lactate (42), whereas members of the microbiota can produce both isomers (43). Little is known about changes in short-chain fatty acids and lactate during human salmonellosis. Of note, patients with noninfectious diarrhea exhibit increased L-lactate levels in the feces (44). Increases in fecal L-lactate in ulcerative colitis are due to augmented excretion by the mucosa (45). In patients with ulcerative colitis suffering from pancolitis and active Crohn's disease, the average fecal L-lactate concentration exceeds 10 mM, whereas it is less than 4 mM in quiescent patients (44).

Here, we report that induction of the *S. Typhimurium* L-lactate dehydrogenase LldD *in vitro* occurred at L-lactate concentrations that span the experimentally determined *in vivo* lactate concentrations. In contrast, exposure to D-lactate had little effect on *lldD* transcription. Consistent with the idea that L-lactate utilization is an adaptation to the environment of the inflamed gut, the D-lactate dehydrogenase Dld was not inducible by oxygen, nitrate, or L-lactate. Furthermore, Dld activity does not provide a fitness advantage in the murine gut (19).

Unlike the cytoplasmic lactate dehydrogenase LdhA used during fermentation, LldD is membrane bound and donates electrons directly to the quinone pool (46). In the murine gut, oxygen likely is the terminal electron acceptor for *S. Typhimurium* L-lactate utilization (19). Our data showed that oxygen availability and aerobic respiration modulated L-lactate utilization genes *in vitro*. Signaling through the respiration-responsive regulatory system ArcAB was required for repression under anaerobic conditions, when electron acceptors are not available for coupling with L-lactate conversion to pyruvate. Similarly, the activity of the terminal oxidase CydAB was essential for expression of L-lactate utilization genes under microaerobic conditions. This shows a dual function for CydAB during lactate oxidation, which serves as the terminal electron acceptor and modulates the electron flux that relieves ArcAB-mediated repression of L-lactate utilization genes. Taken together, our study demonstrates that sensing of host-derived metabolites provides an important cue for a dynamic transcriptional program that benefits *S. Typhimurium* in the murine gut through lactate oxidation and, thus, ensures successful *S. Typhimurium* outgrowth.



**TABLE 1** Bacterial strains and plasmids used in this study

Strain or plasmid identifier	Description	Source or reference
<b>S. Typhimurium strains</b>		
IR715	Nalidixic acid-resistant strain of <i>Salmonella enterica</i> serovar Typhimurium 14028S	53
AJB715	IR715 <i>phoN</i> ::Kan <sup>r</sup>	54
CG6	IR715 $\Delta$ <i>lldD</i>	19
CG124	IR715 $\Delta$ <i>cydA</i>	19
CG200	IR715 $\Delta$ <i>lldR</i>	This study
CG226	IR715 $\Delta$ <i>lldP</i>	This study
CG254	IR715 <i>lldD</i> ::pCG254	This study
CG267	IR715 $\Delta$ <i>arcA lldD</i> ::pCG254	This study
CG268	IR715 $\Delta$ <i>arcB lldD</i> ::pCG254	This study
CG270	IR715 $\Delta$ <i>cydA lldD</i> ::pCG254	This study
MW118	IR715 $\Delta$ <i>arcB</i>	This study
MW119	IR715 $\Delta$ <i>arcA</i>	This study
<b>E. coli strains</b>		
DH5 $\alpha$ $\lambda$ <i>pir</i>	F <sup>-</sup> <i>endA1 hsdR17</i> (r <sub>K</sub> <sup>-</sup> m <sub>K</sub> <sup>+</sup> ) <i>supE44 thi-1 recA1 gyrA relA1</i> $\Delta$ ( <i>lacZYA-argF</i> )U169 $\phi$ 80d <i>lacZ</i> $\Delta$ M15 $\lambda$ <i>pir</i>	55
S17-1 $\lambda$ <i>pir</i>	<i>zxx</i> ::RP4 2-(Tet <sup>r</sup> ::Mu) (Kan <sup>r</sup> ::Tn7) $\lambda$ <i>pir</i>	56
<b>Plasmids</b>		
pRDH10	<i>ori</i> (R6K) <i>mobRP4</i> Cm <sup>r</sup> Tet <sup>r</sup> <i>sacRB</i>	54
pFUSE	<i>ori</i> (R6K) <i>mobRP4</i> Cm <sup>r</sup> <i>lacZYA</i>	57
pCG226	Upstream and downstream regions of <i>S. Typhimurium lldP</i> in pRDH10	This study
pCG254	Fragment of <i>lldD</i> in pFUSE	This study
pCG200	Upstream and downstream regions of <i>S. Typhimurium lldR</i> in pRDH10	This study
pMW195	Upstream and downstream regions of <i>S. Typhimurium arcA</i> in pRDH10	This study
pMW89	Upstream and downstream regions of <i>S. Typhimurium arcB</i> in pRDH10	This study

**MATERIALS AND METHODS**

**Bacterial strains, plasmids, and primers.** All bacterial strains and plasmids used in this study are listed in Table 1. All primers are listed in Tables 2 and 3. *S. Typhimurium* and *E. coli* strains were routinely grown in lysogeny broth (LB; 10 g/liter tryptone, 5 g/liter yeast extract, 10 g/liter sodium chloride) and on LB plates (10 g/liter tryptone, 5 g/liter yeast extract, 10 g/liter sodium chloride, 15 g/liter agar) under aerobic conditions at 37°C. Nalidixic acid (Nal), kanamycin (Kan), and chloramphenicol (Cm) were added to the media as needed at a concentration of 50 mg/liter, 100 mg/liter, and 15 mg/liter, respectively. 5-Bromo-4-chloro-3-indolylphosphate (X-phos; Chem-Impex) was added to the plates to detect the activity of the acidic phosphatase PhoN. All plasmids used were created by use of a Gibson Assembly cloning kit (New England Biolabs). To generate pCG200, pCG226, pMW195, and pMW89, the upstream and downstream regions of the gene of interest were amplified using Q5 HotStart high-fidelity DNA polymerase (New England Biolabs). The upstream and downstream regions were then inserted into SphI-digested pRDH10 using the Gibson Assembly reaction. All plasmids were sequenced to check for point mutations prior to mutagenesis. For cloning experiments, the host for suicide plasmids was DH5 $\alpha$   $\lambda$ *pir*. S17-1  $\lambda$ *pir* served as the donor strain for conjugation into *S. Typhimurium*. After conjugation, single crossovers were selected with LB plates supplemented with Cm. Counterselection was performed by plating on sucrose plates (5% sucrose, 15 g/liter agar, 8 g/liter nutrient broth base) to check for second crossover events. This cloning strategy generates clean, unmarked deletions and was used to create strains CG200, CG226, MW118, and MW119. To generate pCG254, 379 nucleotides of the 3' end of the *lldD* coding sequence (including the stop codon) and 31 nucleotides immediately downstream of the

**TABLE 2** Primers and RT-qPCR parameters

Target	Sequences	Limit of quantification (C <sub>T</sub> value)	Linear dynamic range (no. of copies/ $\mu$ l)	Source or reference
<i>lldP</i>	5'-TGCTGGCGTTCGCGTTTATC-3', 5'-CTCTCTACAGGCTACCGCGG-3'	38	2.69 $\times$ 10 <sup>8</sup> -2.7	This study
<i>lldR</i>	5'-ACCGCTGCCGACAAAGAGAA-3', 5'-CTTTCATCTGGCGATCGCGG-3'	37	2.69 $\times$ 10 <sup>8</sup> -2.7	This study
<i>lldD</i>	5'-TCCGTAACGGGCTGGATGTC-3', 5'-GAAGTTCGCATGACCCTGA-3'	33	2.69 $\times$ 10 <sup>8</sup> -2.7	This study
<i>dld</i>	5'-CCGGAGCAGATCCTGAGCAA-3', 5'-TTTGAATCTTCGGCTGCGC-3'	37	2.10 $\times$ 10 <sup>8</sup> -2.1	This study
<i>gmk</i>	5'-TTGGCAGGGAGGCGTTT-3', 5'-GCGCGAAGTGCCGTAGTAAT-3'	34	2.27 $\times$ 10 <sup>9</sup> -22.7	58
16S rRNA	5'-CAGAAGAAGCACCGGCTAACTC-3', 5'-GCGCTTTACGCCAGTAATT-3'	33	7.21 $\times$ 10 <sup>7</sup> -72.1	58
<i>Cxcl1</i>	5'-TGCACCCAAACCGAAGTCAT-3', 5'-TTGTGACAGGCCAGCGTTTAC-3'	32	4.86 $\times$ 10 <sup>7</sup> -48.6	59
<i>Nos2</i>	5'-TTGGGTCTTGTCTACTCCACGG-3', 5'-CCTCTTTCAGGTCACTTTGGTAGG-3'	37	1.04 $\times$ 10 <sup>8</sup> -1.04 $\times$ 10 <sup>2</sup>	60
<i>Tnf</i>	5'-AGCCAGGAGGGAGAACAAAC-3', 5'-CCAGTGAGTGAAGGGACAGAAC-3'	40	3.2 $\times$ 10 <sup>7</sup> -32	61
<i>Gapdh</i>	5'-TGTAGACCATGTAGTTGAGGTCA-3', 5'-AGGTCGGTGTGAACGGATTG-3'	40	2.31 $\times$ 10 <sup>8</sup> -2.31 $\times$ 10 <sup>2</sup>	59

**TABLE 3** Primers for mutagenesis

Target/purpose	Sequences	Source or reference
Deletion of <i>S. Typhimurium lldR</i>	5'-GCCATCTCCTTGCATGTAAACGTTCCGGTACCGTATC-3', 5'-GTTTTAACCTGGATGATTCGGTGAATGATTATTCA-3', 5'-TTCCGTGAATGATTATTCAGCAGCCAGCGATTATC-3', 5'-GTCGGCTGAACGGTCGCCATGCACCATTCTTG-3'	This study
Deletion of <i>S. Typhimurium arcA</i>	5'-GCCATCTCCTTGCATGCACCGTGCCTAACGAGCGCG-3', 5'-TTTGCGCCTGGGCCGAAAAATTGCCA-3', 5'-GGGCCGAAAAATTGCCAACTAAATCGAAAC-3', 5'-CGTATTGTGACAGCCAGCATGCACCATTCTTG-3'	This study
Deletion of <i>S. Typhimurium arcB</i>	5'-GCCATCTCCTTGCATGTCCACAACGATATCATCAACCGGG-3', 5'-ACCCCGGTCAAACCGGGGTTCTTCAC-3', 5'-AACCGGGTTCCTTACCACAACCTTC-3', 5'-GAAATAGGCCAGATAGCGTTGCATGCACCATTCTTG-3'	This study
Deletion of <i>S. Typhimurium lldP</i>	5'-GGGCGCCATCTCCTTGCATGTGGAAGAAGCAAACACTTATAC-3', 5'-GTTCTCAGGAGACCTGCATTGTGATGCC-3', 5'-GAGACCTGCATTGTGATGCCAAAACGCC-3', 5'-CGGAACAACACCAGGCAGCATGCACCATTCTTGCGGC-3'	This study
Creation of pCG254	5'-GCCGCTCTAGAAGTGTGATGCCCGGTGTCGAATCACGGCGG-3', 5'-CTTTATGTAAGTGCCTGACCGGGAATCCGATCCGACAAC-3'	This study

stop codon were amplified and cloned into *Sma*I-digested pFUSE. pCG254 was conjugated into IR715, CG124, MW119, and MW118 as described above to generate the *lldD* transcriptional fusion in strains CG254, CG270, CG267, and CG268, respectively.

**Quantification of mRNA during growth in mucin broth.** About 100 mg of mucin (porcine stomach type II; Sigma) was suspended in 1 ml ethanol, and the mixture was incubated at room temperature overnight. The ethanol was evaporated in a vacuum centrifuge at 30°C. Dried mucin was resuspended in no-carbon E medium (0.2 g/liter MgSO<sub>4</sub>·7H<sub>2</sub>O, 3.9 g/liter KH<sub>2</sub>PO<sub>4</sub>, 5.0 g/liter anhydrous K<sub>2</sub>HPO<sub>4</sub>, 3.5 g/liter NaNH<sub>4</sub>HPO<sub>4</sub>·4H<sub>2</sub>O) (47, 48) at a final concentration of 0.5% (wt/vol) mucin. Other compounds were dissolved in water and filter sterilized (pore size, 0.2 μm) prior to addition to the complete mucin broth. Sodium L-lactate (Sigma) and sodium nitrate (Sigma) were added to the media as specified for a final concentration of 20 mM and 40 mM, respectively. All media were preincubated in an anaerobic chamber (5% hydrogen, 5% CO<sub>2</sub>, 90% nitrogen; Sheldon Manufacturing) 1 day prior to inoculation. Five milliliters of medium was inoculated with 100 μl of an overnight culture of the strains of interest. The cultures were grown for 3 h in the anaerobic chamber (no electron acceptor condition and nitrate condition) or a hypoxic cabinet (1% oxygen, 99% nitrogen; Coy Laboratory Products), as indicated in each figure legend. RNA was extracted using with an Aurum total RNA minikit (Bio-Rad) according to the manufacturer's protocol. The RNA was then treated with DNase I (Thermo Fisher) twice according to the manufacturer's instructions prior to analysis by RT-qPCR. RNA samples were stored at -80°C.

**Preparation of cDNA and qPCR.** cDNA was prepared using TaqMan reverse transcription reagents (Thermo Fisher) as described by the manufacturer. Briefly, the reaction mixture was prepared using 2.5 μl of 10× RT-PCR buffer, 5.5 μl MgCl<sub>2</sub> (25 mM), 5 μl of deoxynucleoside triphosphates (2.5 mM each), 1.25 μl of random hexamers (50 μM), 1 μl RNase inhibitor, 0.625 μl of reverse transcriptase, and 9.6 μl of template RNA. The RNA concentration and the A<sub>260</sub>/A<sub>280</sub> ratio were evaluated. For bacterial RNA samples, a reaction with RT-PCR buffer, water, and template RNA (no reverse transcriptase) was performed to quantify contamination with DNA. Samples with more than 5% DNA contamination were excluded from analysis. The reverse transcription reaction was performed using the following protocol: 10 min at 25°C, 30 min at 48°C, 5 min at 95°C, and 4°C indefinitely. cDNA and no-reverse-transcription controls were stored at -20°C prior to analysis.

qPCR was performed using SYBR Green (Thermo Fisher) with 2 μl of template DNA and 250 nM each primer in a final reaction volume of 11 μl. The primer sequences and important experimental parameters are listed in Table 2. qPCR was performed using a QuantStudio 6 Flex instrument (Thermo Fisher) with the vendor-supplied, standard SYBR green qPCR protocol. Unless indicated otherwise, the ramp speed was 1.6°C/s. The hold stage was at 50°C for 2 min and 95°C for 10 min. The amplification stage consisted of two steps, 95°C for 15 s and 60°C for 1 min, which were repeated for a total of 40 times. The melt curve was determined by increasing the temperature from 60°C to 95°C at a speed of 0.05°C/s. A nontemplate control (water) was run in addition to the samples. Two technical replicates per biological replicate were assayed. Melt curves for each reaction were evaluated prior to analysis. Data were analyzed using QuantStudio real-time PCR software (v1.2). Baselines were determined using the baseline threshold algorithm. Data were further analyzed using the comparative threshold cycle (C<sub>T</sub>) method for Fig. 1 and 4 and for Fig. S1 and S3 in the supplemental material in Microsoft Excel software (49). PCR fragments containing known concentrations of the qPCR target were used to determine the limit of quantification (the C<sub>T</sub> value for the lowest value in the linear dynamic range), the linear dynamic range, and the efficiency of the qPCR for bacterial targets. Serial dilutions of plasmids containing the gene of interest were used to quantify the absolute counts of the target gene in Fig. S4 and to perform quality control analysis for the qPCR assay (50).

**β-Galactosidase assays.** Five milliliters of LB supplemented with various concentrations of L- or D-lactate (Sigma) was preincubated in the anaerobic chamber 1 day prior to inoculation. Overnight

cultures were grown in the anaerobic chamber (Fig. 2B and C and S2) or aerobically with shaking (Fig. 2A and 3A). The prereduced medium was inoculated with 100  $\mu$ l of overnight culture and incubated in the anaerobic chamber (no electron acceptor conditions) or hypoxic cabinet (1% or 8% oxygen conditions) as indicated for 135 min (Fig. 2A and 3A) or 5 h (Fig. 2B and C and S2). At the end of incubation, cultures were placed on ice for 20 min and  $\beta$ -galactosidase assays were performed based on the protocol described by Miller (51). Briefly, the optical density at 600 nm ( $OD_{600}$ ) of the chilled cultures was taken. One hundred microliters or 500  $\mu$ l of chilled culture was added to 900  $\mu$ l or 500  $\mu$ l of phosphate-buffered saline (PBS), respectively. Bacterial cells were lysed with 20  $\mu$ l of 0.1% SDS and 40  $\mu$ l of chloroform, vortexed for 10 s, and incubated at room temperature for 5 min. Two hundred microliters of 4 mg/ml *o*-nitrophenyl- $\beta$ -D-galactoside (ONPG; Thermo Scientific) was then added to the reaction mixture. After sufficient yellow color had developed, the reaction was stopped with 500  $\mu$ l of 1 M  $Na_2CO_3$  and the time was recorded. The  $A_{420}$  and  $A_{550}$  were taken, and the Miller units were calculated according to the following equation: relative activity (in Miller units) =  $1,000 \times \{[A_{420} - (1.75 \times A_{550})]/(t \times v \times OD_{600})\}$ , where  $t$  is time in minutes and  $v$  is volume in milliliters.

**Mouse experiments.** Conventional C57BL/6 and Swiss Webster mice, originally obtained from The Jackson Laboratory, were bred under specific-pathogen-free conditions in a barrier facility at UT Southwestern. Both male and female mice (age, 6 to 8 weeks) were used for the experiments, and no marked differences between male and female mice were observed. All mice were on a 12-h light/12-h dark cycle and consumed food (Envigo 2919, Teklad Global 16% protein diet, irradiated) and water *ad libitum*. All experiments were conducted in accordance with the policies of the Institutional Animal Care and Use Committee at UT Southwestern.

**Streptomycin-treated mouse model of salmonellosis.** Wild-type C57BL/6 mice were intragastrically treated with 20 mg of sterile streptomycin sulfate (lot number 1796C493; VWR) in water or mock treated with water. One day later, the mice were infected intragastrically with  $1 \times 10^5$  CFU of *S. Typhimurium* strains or mock treated with LB. Mice were euthanized 5 days after infection. The cecal content and cecal tissue were flash frozen in liquid nitrogen for RNA extraction and stored at  $-80^\circ C$ . For analysis of the cecal content by GC-MS, the cecal content was placed in sterile PBS for further analysis.

**Swiss Webster mouse model of salmonellosis.** Wild-type Swiss Webster mice were intragastrically inoculated with  $1 \times 10^9$  CFU of *S. Typhimurium* by using  $5 \times 10^8$  CFU of each strain. Mice were sacrificed at 8 days after infection, and colonic and cecal contents and tissues were collected for analysis. Colonic and cecal contents were placed in sterile PBS, vortexed, and serially diluted on selective agar to determine the number of CFU per gram of each strain. Competitive indices were calculated by dividing the number of CFU per gram of the wild-type strain by the number of CFU per gram of the mutant strain, corrected by the same ratio in the inoculum. Cecal tissue was flash frozen for later analysis and stored at  $-80^\circ C$ .

**RNA extraction from cecal content.** Cecal content was collected, flash frozen in liquid nitrogen, and stored at  $-80^\circ C$ . RNA was extracted with the TRI reagent (Molecular Research Center). Briefly, frozen samples were resuspended in 0.5 ml of TRI reagent and homogenized in a Mini-BeadBeater (BioSpec Products) twice for 30 s each time. Chloroform (0.1 ml) was then added to the tube, and the tube was shaken and incubated for 5 min at room temperature. The samples were then centrifuged at  $12,000 \times g$  for 15 min at  $4^\circ C$ . The aqueous-phase supernatant (0.2 ml) was transferred to a new tube. RNA was precipitated by adding 0.25 ml of isopropanol, followed by incubation at room temperature for 10 min. Samples were then centrifuged at  $12,000 \times g$  for 8 min at  $25^\circ C$  to pellet the RNA. The pellet was then washed with 0.5 ml of 75% ethanol and centrifuged at  $12,000 \times g$  for 5 min at  $25^\circ C$ . The pellet was then air dried and resuspended in DNase/RNase-free water. RNA preparations were then treated twice with DNase I (Ambion) prior to use. cDNA preparation and qPCR were performed as described above.

**GC-MS quantification of lactate.** Lactate measurements were performed as described previously (19, 52). Cecal contents were collected and placed into sterile PBS. Samples were vortexed for 2 min and centrifuged at  $6,000 \times g$  at  $4^\circ C$  for 15 min. Supernatant was then aliquoted and 50  $\mu$ M deuterated lactate (sodium L-lactate-3,3,3- $d_3$ ; CDN Isotopes) was added as the internal standard. Samples were then evaporated to dryness in a vacuum centrifuge and stored at  $-80^\circ C$  prior to analysis. Standards were prepared in the same way as the samples with set concentrations of deuterated and nondeuterated lactate. Samples were then resuspended in pyridine (Sigma), sonicated for 1 min, and incubated at  $80^\circ C$  for 20 min. Samples were derivatized with *N*-tert-butyltrimethylsilyl-*N*-methyltrifluoroacetamide with 1% tert-butyltrimethylchlorosilane (Sigma) and incubated for 1 h at  $80^\circ C$ . Samples were then centrifuged at  $16,000 \times g$  for 1 min to remove the debris, and 80  $\mu$ l of supernatant was transferred to autosampler vials. Analysis was performed using a Shimadzu TQ8040 triple-quadrupole GC-MS. The injection temperature was  $250^\circ C$  with a split ratio of 1:100 and a volume of 1  $\mu$ l. An Rtx-5 SIIIMS fused-silica capillary column was used with helium as the carrier gas (velocity, 50 cm/s). The oven temperature began at  $50^\circ C$  for 2 min and rose to  $100^\circ C$  in increments of  $20^\circ C$  per minute, with a hold at  $100^\circ C$  for 3 min. The oven temperature was then increased to a final temperature of  $330^\circ C$ , rising in increments of  $40^\circ C$  per minute with a final hold for 3 min. The ion source was used in electron ionization mode (70 V, 150  $\mu$ A,  $200^\circ C$ ). Selected ion monitoring (SIM) and multiple-reaction monitoring (MRM) were used, with the event time being 50 ms. The following mass spectrometry parameters were used: for lactate- $d_3$ , an MRM of  $264 > 236$  and a collision energy (CE) of 6 V or an MRM of  $264 > 189$  and a CE of 8 V, and for lactate, an MRM of  $261 > 233$  and a CE of 6 V or an MRM of  $261 > 189$  and a CE of 8 V. The  $m/z$  used for quantification is italicized. The recovery of each sample was calculated using the recovery of internal deuterated standards.

**Cytokine mRNA quantification from cecal tissue.** Inflammatory cytokines were assessed as previously described (19). Flash-frozen tissue was homogenized with a Mini-BeadBeater (BioSpec Products). RNA was extracted with the TRI reagent (Molecular Research Center) according to the manufacturer's

instructions. RNA was treated with DNase I (Thermo Fisher) following extraction. cDNA preparation and qPCR were then performed as described above.

**Statistical analysis.** Data analysis was done in Microsoft Excel (v16.15.5) and GraphPad Prism (v7.0c) software. All data were transformed with the natural logarithm (ln) prior to analysis. The normality of all transformed data was tested using the D'Agostino-Pearson test (for sample sizes of 8 or more) or the Shapiro-Wilk test (for less than 8 samples). Data for mice that were euthanized for health reasons prior to the end of the experiment were excluded from analysis. To determine statistical differences between groups of mice, a two-tailed, unpaired Student's *t* test was applied to the logarithmically transformed data. To determine statistical differences between wild-type and mutant bacterial populations within the same animal (competition experiments), a two-tailed, paired Student's *t* test was used. *P* values of less than 0.05 were considered significant.

## SUPPLEMENTAL MATERIAL

Supplemental material for this article may be found at <https://doi.org/10.1128/IAI.00773-18>.

**SUPPLEMENTAL FILE 1**, PDF file, 0.2 MB.

## ACKNOWLEDGMENTS

Work in S.E.W.'s lab was funded by the NIH (AI118807, AI128151), the Welch Foundation (I-1858), the Burroughs Wellcome Fund (1017880), and a research scholar grant (RSG-17-048-01-MPC) from the American Cancer Society. C.C.G. received an NSF graduate research fellowship (1000194723). R.B.C. was funded by an NIH training grant (GM109776). W.Z. was supported by a research fellows award from the Crohn's and Colitis Foundation of America (454921).

The funders had no role in study design, data collection and interpretation, or the decision to submit the work for publication. Any opinions, findings, and conclusions or recommendations expressed in this material are those of the authors and do not necessarily reflect the views of the funding agencies.

We thank Julie Pfeiffer, David Hendrixson, Ezra Burstein, and Vanessa Sperandio for their advice and comments.

S.E.W. is listed as an inventor on patent application WO2014200929A1, which describes a treatment to prevent the inflammation-associated expansion of *Enterobacteriaceae*. The other authors have no additional financial interests.

## REFERENCES

- Santos RL, Raffatellu M, Bevins CL, Adams LG, Tukul C, Tsois RM, Baumler AJ. 2009. Life in the inflamed intestine, *Salmonella* style. *Trends Microbiol* 17:498–506. <https://doi.org/10.1016/j.tim.2009.08.008>.
- Mills DM, Bajaj V, Lee CA. 2006. A 40 kb chromosomal fragment encoding *Salmonella typhimurium* invasion genes is absent from the corresponding region of the *Escherichia coli* K-12 chromosome. *Mol Microbiol* 15:749–759. <https://doi.org/10.1111/j.1365-2958.1995.tb02382.x>.
- Galan JE, Curtiss R. 1989. Cloning and molecular characterization of genes whose products allow *Salmonella typhimurium* to penetrate tissue culture cells. *Proc Natl Acad Sci U S A* 86:6383–6387. <https://doi.org/10.1073/pnas.86.16.6383>.
- Jones BD, Ghori N, Falkow S. 1994. *Salmonella typhimurium* initiates murine infection by penetrating and destroying the specialized epithelial M cells of the Peyer's patches. *J Exp Med* 180:15–23. <https://doi.org/10.1084/jem.180.1.15>.
- Shea JE, Hensel M, Gleeson C, Holden DW. 1996. Identification of a virulence locus encoding a second type III secretion system in *Salmonella typhimurium*. *Proc Natl Acad Sci U S A* 93:2593–2597.
- Vazquez-Torres A, Xu Y, Jones-Carson J, Holden DW, Lucia SM, Dinauer MC, Mastroeni P, Fang FC. 2000. *Salmonella* pathogenicity island 2-dependent evasion of the phagocyte NADPH oxidase. *Science* 287:1655–1658.
- Coburn B, Li Y, Owen D, Vallance BA, Finlay BB. 2005. *Salmonella enterica* serovar Typhimurium pathogenicity island 2 is necessary for complete virulence in a mouse model of infectious enterocolitis. *Infect Immun* 73:3219–3227. <https://doi.org/10.1128/IAI.73.6.3219-3227.2005>.
- Coombes BK, Coburn BA, Potter AA, Gomis S, Mirakhor K, Li Y, Finlay BB. 2005. Analysis of the contribution of *Salmonella* pathogenicity islands 1 and 2 to enteric disease progression using a novel bovine ileal loop model and a murine model of infectious enterocolitis. *Infect Immun* 73:7161–7169. <https://doi.org/10.1128/IAI.73.11.7161-7169.2005>.
- Tsois RM, Adams LG, Ficht TA, Baumler AJ. 1999. Contribution of *Salmonella typhimurium* virulence factors to diarrheal disease in calves. *Infect Immun* 67:4879–4885.
- Stecher B, Robbani R, Walker AW, Westendorf AM, Barthel M, Kremer M, Chaffron S, Macpherson AJ, Buer J, Parkhill J, Dougan G, von Mering C, Hardt WD. 2007. *Salmonella enterica* serovar Typhimurium exploits inflammation to compete with the intestinal microbiota. *PLoS Biol* 5:2177–2189. <https://doi.org/10.1371/journal.pbio.0050244>.
- Barman M, Unold D, Shifley K, Amir E, Hung K, Bos N, Salzman N. 2008. Enteric salmonellosis disrupts the microbial ecology of the murine gastrointestinal tract. *Infect Immun* 76:907–915. <https://doi.org/10.1128/IAI.01432-07>.
- Lawley TD, Bouley DM, Hoy YE, Gerke C, Relman DA, Monack DM. 2008. Host transmission of *Salmonella enterica* serovar Typhimurium is controlled by virulence factors and indigenous intestinal microbiota. *Infect Immun* 76:403–416. <https://doi.org/10.1128/IAI.01189-07>.
- Rivera-Chavez F, Zhang LF, Faber F, Lopez CA, Byndloss MX, Olsan EE, Xu G, Velazquez EM, Lebrilla CB, Winter SE, Baumler AJ. 2016. Depletion of butyrate-producing Clostridia from the gut microbiota drives an aerobic luminal expansion of *Salmonella*. *Cell Host Microbe* 19:443–454. <https://doi.org/10.1016/j.chom.2016.03.004>.
- Lopez CA, Rivera-Chavez F, Byndloss MX, Baumler AJ. 2015. The periplasmic nitrate reductase NapABC supports luminal growth of *Salmonella enterica* serovar Typhimurium during colitis. *Infect Immun* 83:3470–3478. <https://doi.org/10.1128/IAI.00351-15>.
- Lopez CA, Winter SE, Rivera-Chavez F, Xavier MN, Poon V, Nuccio SP, Tsois RM, Baumler AJ. 2012. Phage-mediated acquisition of a type III

- secreted effector protein boosts growth of salmonella by nitrate respiration. *mBio* 3:e00143-12. <https://doi.org/10.1128/mBio.00143-12>.
16. Wintner SE, Thiennimitr P, Wintner MG, Butler BP, Huseby DL, Crawford RW, Russell JM, Bevins CL, Adams LG, Tsois RM, Roth JR, Baumler AJ. 2010. Gut inflammation provides a respiratory electron acceptor for *Salmonella*. *Nature* 467:426–429. <https://doi.org/10.1038/nature09415>.
  17. Spiga L, Wintner MG, Furtado de Carvalho T, Zhu W, Hughes ER, Gillis CC, Behrendt CL, Kim J, Chessa D, Andrews-Polymenis HL, Beiting DP, Santos RL, Hooper LV, Wintner SE. 2017. An oxidative central metabolism enables *Salmonella* to utilize microbiota-derived succinate. *Cell Host Microbe* 22:291–301.e6. <https://doi.org/10.1016/j.chom.2017.07.018>.
  18. Thiennimitr P, Wintner SE, Wintner MG, Xavier MN, Tolstikov V, Huseby DL, Sterzenbach T, Tsois RM, Roth JR, Baumler AJ. 2011. Intestinal inflammation allows *Salmonella* to use ethanolamine to compete with the microbiota. *Proc Natl Acad Sci U S A* 108:17480–17485. <https://doi.org/10.1073/pnas.1107857108>.
  19. Gillis CC, Hughes ER, Spiga L, Wintner MG, Zhu W, Furtado D, Carvalho T, Chanin RB, Behrendt CL, Hooper LV, Santos RL, Wintner SE. 2018. Dysbiosis-associated change in host metabolism generates lactate to support *Salmonella* growth. *Cell Host Microbe* 23:54–64.e6. <https://doi.org/10.1016/j.chom.2017.11.006>.
  20. Kelly CJ, Zheng L, Campbell EL, Saeedi B, Scholz CC, Bayless AJ, Wilson KE, Glover LE, Kominsky DJ, Magnuson A, Weir TL, Ehrentraut SF, Pickel K, Kuhn KA, Lanis JM, Nguyen V, Taylor CT, Colgan SP. 2015. Crosstalk between microbiota-derived short-chain fatty acids and intestinal epithelial HIF augments tissue barrier function. *Cell Host Microbe* 17:662–671. <https://doi.org/10.1016/j.chom.2015.03.005>.
  21. Donohoe DR, Wali A, Brylawski BP, Bultman SJ. 2012. Microbial regulation of glucose metabolism and cell-cycle progression in mammalian colonocytes. *PLoS One* 7:e46589. <https://doi.org/10.1371/journal.pone.0046589>.
  22. Byndloss MX, Olsan EE, Rivera-Chávez F, Tiffany CR, Cevallos SA, Lokken KL, Torres TP, Byndloss AJ, Faber F, Gao Y, Litvak Y, Lopez CA, Xu G, Napoli E, Giulivi C, Tsois RM, Revzin A, Lebrilla CB, Bäuml AJ. 2017. Microbiota-activated PPAR- $\gamma$  signaling inhibits dysbiotic *Enterobacteriaceae* expansion. *Science* 357:570–575. <https://doi.org/10.1126/science.aam9949>.
  23. Aguilera L, Campos E, Gimenez R, Badia J, Aguilar J, Baldoma L. 2008. Dual role of *l*ldR in regulation of the *l*ldPRD operon, involved in *l*-lactate metabolism in *Escherichia coli*. *J Bacteriol* 190:2997–3005. <https://doi.org/10.1128/JB.02013-07>.
  24. Reference deleted.
  25. Dong JM, Taylor JS, Latour DJ, Iuchi S, Lin EC. 1993. Three overlapping *lct* genes involved in *l*-lactate utilization by *Escherichia coli*. *J Bacteriol* 175:6671–6678.
  26. Iuchi S, Aristarkhov A, Dong JM, Taylor JS, Lin EC. 1994. Effects of nitrate respiration on expression of the *Arc*-controlled operons encoding succinate dehydrogenase and flavin-linked *l*-lactate dehydrogenase. *J Bacteriol* 176:1695–1701.
  27. Hong JS, Kaback HR. 1972. Mutants of *Salmonella typhimurium* and *Escherichia coli* pleiotropically defective in active transport. *Proc Natl Acad Sci U S A* 69:3336–3340.
  28. Evans MR, Fink RC, Vazquez-Torres A, Porwollik S, Jones-Carson J, McClelland M, Hassan HM. 2011. Analysis of the *ArcA* regulon in anaerobically grown *Salmonella enterica* sv. *Typhimurium*. *BMC Microbiol* 11:58. <https://doi.org/10.1186/1471-2180-11-58>.
  29. Lynch AS, Lin EC. 1996. Transcriptional control mediated by the *ArcA* two-component response regulator protein of *Escherichia coli*: characterization of DNA binding at target promoters. *J Bacteriol* 178:6238–6249.
  30. Iuchi S, Lin EC. 1988. *arcA* (dye), a global regulatory gene in *Escherichia coli* mediating repression of enzymes in aerobic pathways. *Proc Natl Acad Sci U S A* 85:1888–1892.
  31. Georgellis D, Kwon O, Lin EC. 2001. Quinones as the redox signal for the *arc* two-component system of bacteria. *Science* 292:2314–2316. <https://doi.org/10.1126/science.1059361>.
  32. Day DW, Mandal BK, Morson BC. 1978. The rectal biopsy appearances in *Salmonella colitis*. *Histopathology* 2:117–131.
  33. McGovern VJ, Slavutin LJ. 1979. Pathology of salmonella colitis. *Am J Surg Pathol* 3:483–490.
  34. Harris JC, Dupont HL, Hornick RB. 1972. Fecal leukocytes in diarrheal illness. *Ann Intern Med* 76:697–703.
  35. Alvarado T. 1983. Faecal leucocytes in patients with infectious diarrhoea. *Trans R Soc Trop Med Hyg* 77:316–320.
  36. Barthel M, Hapfelmeier S, Quintanilla-Martínez L, Kremer M, Rohde M, Hogardt M, Pfeffer K, Rüssmann H, Hardt W-D. 2003. Pretreatment of mice with streptomycin provides a *Salmonella enterica* serovar Typhimurium colitis model that allows analysis of both pathogen and host. *Infect Immun* 71:2839–2858. <https://doi.org/10.1128/IAI.71.5.2839-2858.2003>.
  37. Nuccio SP, Baumler AJ. 2014. Comparative analysis of *Salmonella* genomes identifies a metabolic network for escalating growth in the inflamed gut. *mBio* 5:e00929-14. <https://doi.org/10.1128/mBio.00929-14>.
  38. McClelland M, Sanderson KE, Clifton SW, Latreille P, Porwollik S, Sabo A, Meyer R, Bieri T, Ozersky P, McLellan M, Harkins CR, Wang C, Nguyen C, Berghoff A, Elliott G, Kohlberg S, Strong C, Du F, Carter J, Kremizki C, Layman D, Leonard S, Sun H, Fulton L, Nash W, Miner T, Minx P, Delehaunty K, Fronick C, Magrini V, Nhan M, Warren W, Florea L, Spieth J, Wilson RK. 2004. Comparison of genome degradation in *Paratyphi A* and *Typhi*, human-restricted serovars of *Salmonella enterica* that cause typhoid. *Nat Genet* 36:1268–1274. <https://doi.org/10.1038/ng1470>.
  39. Tanner JR, Kingsley RA. 2018. Evolution of *Salmonella* within hosts. *Trends Microbiol* 26:986–998. <https://doi.org/10.1016/j.tim.2018.06.001>.
  40. Thomson NR, Clayton DJ, Windhorst D, Vernikos G, Davidson S, Churcher C, Quail MA, Stevens M, Jones MA, Watson M, Barron A, Layton A, Pickard D, Kingsley RA, Bignell A, Clark L, Harris B, Ormond D, Abdellah Z, Brooks K, Cherevach I, Chillingworth T, Woodward J, Norberczak H, Lord A, Arrowsmith C, Jagels K, Moule S, Mungall K, Sanders M, Whitehead S, Chabalgoity JA, Maskell D, Humphrey T, Roberts M, Barrow PA, Dougan G, Parkhill J. 2008. Comparative genome analysis of *Salmonella enteritidis* PT4 and *Salmonella Gallinarum* 287/91 provides insights into evolutionary and host adaptation pathways. *Genome Res* 18:1624–1637. <https://doi.org/10.1101/gr.077404.108>.
  41. Chiu CH, Tang P, Chu C, Hu S, Bao Q, Yu J, Chou YY, Wang HS, Lee YS. 2005. The genome sequence of *Salmonella enterica* serovar *Choleraesuis*, a highly invasive and resistant zoonotic pathogen. *Nucleic Acids Res* 33:1690–1698. <https://doi.org/10.1093/nar/gki297>.
  42. Adeva-Andany M, López-Ojén M, Funcasta-Calderón R, Ameneiros-Rodríguez E, Donapetry-García C, Vila-Altesor M, Rodríguez-Seijas J. 2014. Comprehensive review on lactate metabolism in human health. *Mitochondrion* 17:76–100. <https://doi.org/10.1016/j.mito.2014.05.007>.
  43. Belenguer A, Duncan SH, Holtrop G, Anderson SE, Lobley GE, Flint HJ. 2007. Impact of pH on lactate formation and utilization by human fecal microbial communities. *Appl Environ Microbiol* 73:6526–6533. <https://doi.org/10.1128/AEM.00508-07>.
  44. Hove H, Mortensen PB. 1995. Influence of intestinal inflammation (IBD) and small and large bowel length on fecal short-chain fatty acids and lactate. *Dig Dis Sci* 40:1372–1380.
  45. Hove H, Holtug K, Jeppesen PB, Mortensen PB. 1995. Butyrate absorption and lactate secretion in ulcerative colitis. *Dis Colon Rectum* 38:519–525.
  46. Futai M, Kimura H. 1977. Inducible membrane-bound *l*-lactate dehydrogenase from *Escherichia coli*. Purification and properties. *J Biol Chem* 252:5820–5827.
  47. Vogel HJ, Bonner DM. 1956. Acetylornithinase of *Escherichia coli*: partial purification and some properties. *J Biol Chem* 218:97–106.
  48. Berkowitz D, Hushon JM, Whitfield HJ, Jr, Roth J, Ames BN. 1968. Procedure for identifying nonsense mutations. *J Bacteriol* 96:215–220.
  49. Schmittgen TD, Livak KJ. 2008. Analyzing real-time PCR data by the comparative C(T) method. *Nat Protoc* 3:1101–1108.
  50. Bustin SA, Benes V, Garson JA, Hellemans J, Huggett J, Kubista M, Mueller R, Nolan T, Pfaffl MW, Shipley GL, Vandesompele J, Wittwer CT. 2009. The MIQE guidelines: minimum information for publication of quantitative real-time PCR experiments. *Clin Chem* 55:611–622. <https://doi.org/10.1373/clinchem.2008.112797>.
  51. Miller JH. 1972. Experiments in molecular genetics. Cold Spring Harbor Laboratory, Cold Spring Harbor, NY.
  52. Luethy PM, Huynh S, Ribardo DA, Wintner SE, Parker CT, Hendrixson DR. 2017. Microbiota-derived short-chain fatty acids modulate expression of *Campylobacter jejuni* determinants required for commensalism and virulence. *mBio* 8:e00407-17. <https://doi.org/10.1128/mBio.00407-17>.
  53. Stojiljkovic I, Baumler AJ, Heffron F. 1995. Ethanolamine utilization in *Salmonella typhimurium*: nucleotide sequence, protein expression, and mutational analysis of the *cchA cchB eutE eutJ eutG eutH* gene cluster. *J Bacteriol* 177:1357–1366.
  54. Kingsley RA, Humphries AD, Weening EH, De Zoete MR, Wintner S, Papaconstantinopoulou A, Dougan G, Bäuml AJ. 2003. Molecular and phenotypic analysis of the CS54 island of *Salmonella enterica* serotype *Typhimurium*: identification of intestinal colonization and persistence

- determinants. *Infect Immun* 71:629–640. <https://doi.org/10.1128/IAI.71.2.629-640.2003>.
55. Pal D, Venkova-Canova T, Srivastava P, Chattoraj DK. 2005. Multipartite regulation of *rctB*, the replication initiator gene of *Vibrio cholerae* chromosome II. *J Bacteriol* 187:7167–7175. <https://doi.org/10.1128/JB.187.21.7167-7175.2005>.
56. Simon R, Priefer U, Puhler A. 1983. A broad host range mobilization system for in vivo genetic engineering: transposon mutagenesis in gram negative bacteria. *Nat Biotechnol* 1:784–791. <https://doi.org/10.1038/nbt1183-784>.
57. Baumler AJ, Tsois RM, van der Velden AW, Stojiljkovic I, Anic S, Heffron F. 1996. Identification of a new iron regulated locus of *Salmonella typhi*. *Gene* 183:207–213.
58. Bohez L, Ducatelle R, Pasmans F, Botteldoorn N, Haesebrouck F, Van Immerseel F. 2006. *Salmonella enterica* serovar Enteritidis colonization of the chicken caecum requires the HliA regulatory protein. *Vet Microbiol* 116:202–210. <https://doi.org/10.1016/j.vetmic.2006.03.007>.
59. Overbergh L, Giulietti A, Valckx D, Decallonne R, Bouillon R, Mathieu C. 2003. The use of real-time reverse transcriptase PCR for the quantification of cytokine gene expression. *J Biomol Tech* 14:33–43.
60. Godinez I, Haneda T, Raffatellu M, George MD, Paixao TA, Rolan HG, Santos RL, Dandekar S, Tsois RM, Baumler AJ. 2008. T cells help to amplify inflammatory responses induced by *Salmonella enterica* serotype Typhimurium in the intestinal mucosa. *Infect Immun* 76:2008–2017. <https://doi.org/10.1128/IAI.01691-07>.
61. Hughes ER, Winter MG, Duerkop BA, Spiga L, Furtado de Carvalho T, Zhu W, Gillis CC, Buttner L, Smoot MP, Behrendt CL, Cherry S, Santos RL, Hooper LV, Winter SE. 2017. Microbial respiration and formate oxidation as metabolic signatures of inflammation-associated dysbiosis. *Cell Host Microbe* 21:208–219. <https://doi.org/10.1016/j.chom.2017.01.005>.